JACC: CARDIOVASCULAR INTERVENTIONS VOL. 7, NO. 6, 2014

ISSN 1936-8798/$36.00
PUBLISHED BY ELSEVIER INC. http://dx.doi.org/10.1016/j.jcin.2013.11.023

Coronary and Microvascular Physiology During Intra-Aortic Balloon Counterpulsation

Kalpa De Silva, MBBS, PhD,* Matthew Lumley, MBBS, BSc,* Balrik Kailey, BSc,* Jordi Alastruey, PhD,† Antoine Guilcher, PhD,‡ Kaleab N. Asrress, MA, BM, BCh,* Sven Plein, MD, PhD,†§ Michael Marber, PhD,* Simon Redwood, MBBS, MD,* Divaka Perera, MA, MD*

London, and Leeds, United Kingdom

Objectives This study sought to identify the effect of coronary autoregulation on myocardial perfusion during intra-aortic balloon pump (IABP) therapy.

Background IABP is the most commonly used circulatory support device, although its efficacy in certain scenarios has been questioned. The impact of alterations in microvascular function on IABP efficacy has not previously been evaluated in humans.

Methods Thirteen patients with ischemic cardiomyopathy (left ventricular ejection fraction: 34 ± 8%) undergoing percutaneous coronary intervention were recruited. Simultaneous intracoronary pressure and Doppler-flow measurements were undertaken in the target vessel following percutaneous coronary intervention, during unassisted and IABP-assisted conditions. Coronary autoregulation was modulated by the use of intracoronary adenosine, inducing maximal hyperemia. Wave intensity analysis characterized the coronary wave energies associated with balloon counterpulsation.

Results Two unique diastolic coronary waves were temporally associated with IABP device use; a forward compression wave and a forward expansion wave caused by inflation and deflation, respectively. During basal conditions, IABP therapy increased distal coronary pressure (82.4 ± 16.1 vs. 88.7 ± 17.8 mm Hg, $p = 0.03$), as well as microvascular resistance (2.32 ± 0.52 vs. 3.27 ± 0.41 mm Hg cm s^{-1}, $p = 0.001$), with no change in average peak velocity (30.6 ± 12.0 vs. 26.6 ± 11.3 cm s^{-1}, $p = 0.59$). When autoregulation was disabled, counterpulsation caused an increase in average peak velocity (39.4 ± 10.5 vs. 44.7 ± 17.5 cm s^{-1}, $p = 0.002$) that was linearly related with IABP–forward compression wave energy ($R^2 = 0.71$, $p = 0.001$).

Conclusions Autoregulation ameliorates the effect of IABP on coronary flow. However, during hyperemia, IABP augments myocardial perfusion, principally due to a diastolic forward compression wave caused by balloon inflation, suggesting IABP would be of greatest benefit when microcirculatory reserve is exhausted. (J Am Coll Cardiol Intv 2014;7:631–40) © 2014 by the American College of Cardiology Foundation

From the *King's College London British Heart Foundation Centre of Excellence, National Institute for Health Research Biomedical Research Centre at Guy's and St. Thomas's National Health Service Foundation Trust, Cardiovascular Division, The Rayne Institute, London, United Kingdom; †Department of Biomedical Engineering, Division of Imaging Sciences and Biomedical Engineering, King's College London, King's Health Partners, St. Thomas's Hospital, London, United Kingdom; ‡Department of Clinical Pharmacology, St. Thomas's National Health Service Foundation Trust, London, United Kingdom; and the §Multidisciplinary Cardiovascular Research Centre, Leeds Institute of Genetics, Health and Therapeutics University of Leeds, Leeds, United Kingdom. This research was supported by an unrestricted educational grant from Maquet Cardiovascular. Dr. De Silva has received funding from a Heart Research U.K. fellowship grant (#RG2593/10/12). Dr. Alastruey has received funding from a British Heart Foundation fellowship grant (#FS/09/030/27812), the Centre of Excellence in Medical Engineering (funded by the Wellcome Trust and Engineering and Physical Sciences Research Council under grant #WT 088641/Z/09/Z)

In excess of one-third of all coronary revascularization procedures occur in the context of underlying impaired left ventricular function, with an associated increase in morbidity and mortality (1–3). The intra-aortic balloon pump (IABP) is commonly used during percutaneous coronary intervention (PCI) with the aim of increasing coronary blood flow through augmentation of the diastolic aortocoronary pressure gradient. Additionally, IABP therapy decreases myocardial oxygen demand, by reducing the end-diastolic pressure, and, therefore, the afterload, making it an attractive means of ameliorating ischemia and consequently enhancing cardiac output. However, recent randomized control data, in clinical scenarios where IABP therapy is commonly employed, have shown limited efficacy with routine placement of the device (4–6). The physiological basis for this lack of benefit remains unclear, but it may relate to the interaction of the device with the innate homeostatic coronary autoregulatory mechanisms that govern myocardial perfusion, particularly in regard to the vasomotor control at the level of the microcirculatory resistance vessels. IABP therapy may only provide additional hemodynamic support when myocardial perfusion is outside the normal physiological range, when autoregulation has been pathologically disabled, in conditions such as profound cardiogenic shock or persistent ischemia.

Abbreviations and Acronyms

APV = average peak velocity
BEW = backward expansion waves
DTI = diastolic time index
FCW = forward compression wave
FEW = forward expansion wave
IABP = intra-aortic balloon pump
P_a = aortic pressure
PCI = percutaneous coronary intervention
P_d = intracoronary pressure
TTI = tension time index
WIA = wave intensity analysis

Regional and global left ventricular perfusion and function are closely related to the microvascular integrity of the relevant myocardial territories, with microvascular dysfunction leading to left ventricular impairment and vice versa. The advent of pressure and Doppler sensor-tipped guidewire technology has allowed detailed in vivo interrogation of microcirculatory physiology (7,8). Wave intensity analysis (WIA) of phasic coronary pressure and flow profiles has allowed further characterization of the microcirculation and its impact on coronary flow in a number of stable and acute clinical settings (9–11). These studies demonstrate that mechanical impedance of the coronary microcirculation by the myocardium is the predominant factor that governs myocardial perfusion, with a backward traveling (microcirculatory) expansion wave (BEW), and a forward traveling (aortic) compression wave (FCW) identified as being the most influential in generating diastolic coronary flow (12–14). WIA has not previously been used in humans to assess the effect of IABP counterpulsation therapy on the energy transfer within the coronary circulation.

The aim of this study was to characterize the effects of IABP therapy on the coronary circulation by simultaneously assessing coronary flow, microvascular resistance, and wave energy. Using these indices, we assessed whether microcirculatory autoregulation modulates the effects of IABP therapy in patients with chronic ischemic cardiomyopathy undergoing PCI.

Methods

Study population. Patients scheduled to undergo high-risk single-vessel or multivessel PCI were considered for inclusion in the study. High risk was defined as the presence of impaired left ventricular function (ejection fraction <40% on cardiac magnetic resonance imaging, echocardiography, or left ventricular angiography) and a large amount of myocardium subtended by stenosed vessels, characterized by the BCIS-JS (British Cardiovascular Intervention Society Jeopardy Score) of 6 or greater. The BCIS-JS has been described previously (15), but in brief, it is a modification of the Duke Jeopardy Score (16), which allows broader classification of coronary anatomy, including left main coronary artery stenoses and bypass grafts (the total score ranges from 0 to 12). Exclusion criteria were a prior diagnosis of significant aortic valvular disease, nonischemic cardiomyopathy, severe peripheral artery disease precluding insertion of the IABP catheter, an acute coronary syndrome within the preceding 48 h, or cardiogenic shock.

Cardiac catheterization, IABP, and intracoronary measurement protocol. All patients were preloaded with aspirin (300 mg) and clopidogrel (600 mg). Coronary angiography was performed using a standard Judkins technique via a femoral artery approach. A 40-cc IABP catheter (Maquet Cardiovascular, Rastatt, Germany) was inserted via the contralateral femoral artery and deployed in the descending aorta distal to the left subclavian artery origin at the start of the procedure and counterpulsation was commenced at 1:1 augmentation ratio. Intracoronary nitroglycerin was administered before diagnostic angiography and intracoronary physiological measurements to ensure maximal epicardial arterial vasodilation. Hemodynamic measurements were obtained in the target vessel at least 5 min following final balloon occlusion during PCI. Aortic pressure (P_a) was

and the National Institute for Health Research Biomedical Research Centre at Guy's and St. Thomas's National Health Service Foundation Trust and King's College London. Dr. Plein has received funding from a British Heart Foundation fellowship (FS/1062/28409). Dr. Guilcher is a shareholder in Centron Diagnostics Ltd. Dr. Perera has received financial support from the U.K. Department of Health via the National Institute for Health Research Comprehensive Biomedical Research Centre Award to Guy's and St. Thomas's National Health Service Foundation Trust in partnership with King's College London. All other authors have reported that they have no relationships relevant to the contents of this paper to disclose.

Manuscript received October 16, 2013; revised manuscript received November 11, 2013, accepted November 21, 2013.

measured via the coronary guiding catheter. Intracoronary pressure (P_d) and average peak velocity (APV) were measured via a 0.014-inch dual pressure and Doppler sensor-tipped guidewire (ComboWire, Volcano Corp., San Diego, California), the tip being positioned in the distal vessel. Simultaneous pressure and Doppler measurements were repeated 3× for each condition to reduce acquisition error, ensuring the resumption of steady state between measurements, defined as a return of APV to the baseline value.

First, basal measurements were obtained (with autoregulation "switched on") during 1:1 IABP augmentation. Then, measurements were obtained after transiently disabling autoregulation, with 1:1 IABP augmentation. Autoregulation was disabled by inducing maximal hyperemia via sequentially increasing doses of intracoronary adenosine, with the maximal tolerable dose dictated by the onset of atrioventricular conduction block or systemic symptoms (up to 60 μg were administered in the right and up to 96 μg in the left coronary arteries, respectively). Basal and hyperemic measurements were then repeated in unassisted conditions, after placing the IABP on "stand-by" mode, and allowing at least 4 min for return of basal steady-state conditions.

Data analysis. PHASIC PRESSURE AND FLOW ANALYSIS. Data were sampled at 200 Hz and analyzed off-line, using a customized program developed in Matlab (Mathworks, Inc., Natick, Massachusetts). A Savitzky-Golay convolution method (17) was adopted, using a polynomial filter to refine the derivatives of the P_a and APV signals. Three to 6 consecutive cardiac cycles were selected for resting and hyperemic conditions, gated on the electrocardiographic R-wave peak, with ensemble averaging of P_a, P_d, APV, and heart rate. For the purposes of WIA, it has been considered that diastole commences with the onset of ventricular relaxation, signified by the dicrotic notch on the arterial pressure waveform, as previously described (14). Net coronary wave intensity (δI) was calculated from the time-derivatives (δt) of ensemble-averaged coronary pressure and flow velocity (U) as $\delta I = \delta P_d/\delta t \times \delta U/\delta t$ (10,18). Coincident (microcirculation-derived) backward and (aorta-derived) forward propagating waves were separated assuming blood density to be 1,050 kg/m^3 and estimating coronary wave speed using the sum of squares method (18,19). The peak energies (in W m^{-2} s^{-2} × 10^5) carried by the 3 most prominent wave energies identified were analyzed. These were the positive, aorta-derived FCW, occurring at the onset of systole; the concurrently occurring negative, backward (microcirculation-derived) compression wave, and BEW, the first negative wave occurring at the onset of ventricular relaxation, identified by the onset of diastole. Additionally, the waveforms that were associated with inflation and deflation of the IABP balloon in diastole were also analyzed. Total wave energy (area under the curve) was also determined to identify the relative changes occurring during unassisted and IABP-assisted conditions. The investigators who performed the data analyses were blinded to all clinical patient data.

PULSE-WAVE AND MEAN-PER-BEAT PRESSURE-FLOW ANALYSIS. Pulse wave analysis was performed using custom-made programs (Matlab) in both unassisted and assisted aortic arterial waveforms. The area under the systolic phase of the pressure tracing (tension time index, TTI), and diastolic phase, (diastolic time index, DTI), were determined using the dicrotic notch (Fig. 1). TTI relates to myocardial oxygen demand and DTI to coronary perfusion (20). The Buckberg index was also calculated, providing a ratio of myocardial oxygen supply and demand, which is the quotient of diastolic to systolic pressure-time integral, representing the potential relationship between subendocardial blood supply (DTI) and afterload (TTI), respectively (20). To assess the effect of the IABP device on the timing of the cardiac cycle, diastolic time fraction was calculated. This represents the ratio of time in diastole to duration of a complete heart cycle.

Velocity time integral was calculated as follows:

$$VTI = \sum_{t-start}^{t-end} v_t \times \delta t$$

where t represents time during the cardiac cycle from t_{-start} to t_{-end}, v_t is the instantaneous flow velocity at time t, and δt represents the interval between successive measurements.

Hyperemic and nonhyperemic (basal) microvascular resistance were calculated as the ratio of mean P_d to APV (mm Hg cm s^{-1}) during maximal hyperemia or basal conditions, respectively, obtained through simultaneous intracoronary pressure-flow measurements, during 3 to 6 consecutive cardiac cycles (8,21).

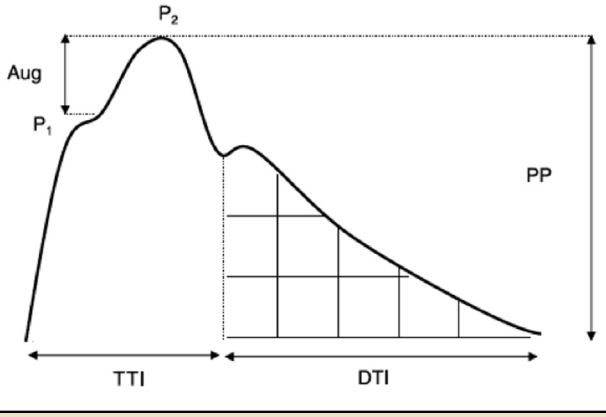

Figure 1. Arterial Pressure Waveform: Pulse Wave Parameters

Two systolic peaks are labeled P_1 and P_2. The area under the curve during systole is the tension time index (TTI) and during diastole is diastolic time index (DTI). Aug = augmentation pressure; PP = pulse pressure.

Statistical analysis. Statistical analysis was performed using IBM SPSS (version 20, Armonk, New York). D'Agostino and Pearson omnibus normality test was performed to ensure a nonskewed distribution. Two-way analysis of variance without replication was performed for each measured variable when comparing to ≥2 different (nominal) conditions. Correlation analysis was used to quantify the relationship between variables. A 2-tail test for significance was performed in all analyses; $p \leq 0.05$ was considered statistically significant. Data are represented as mean ± SD, unless otherwise stipulated.

Ethical approval. The study protocol was approved by the U.K. National Health Service research ethics committee (Reference: 11/H0804/10). All participants were provided with an information sheet detailing the study protocol prior to providing informed verbal and written consent.

Results

Baseline characteristics. Thirteen patients with ischemic cardiomyopathy were recruited, 11 (age 67 ± 11 years) with a left ventricular ejection fraction of 34 ± 8% completed the study protocol. Two patients became hemodynamically compromised during the procedure and did not complete the study protocol and were therefore excluded from the final analysis. Of our study group, 82% (n = 9) were hypertensive, 91% (n = 10) were hypercholesterolemic, and all had prior myocardial infarction. The high-risk nature of this cohort was typified by the elevated logistic EuroSCORE (European System for Cardiac Operative Risk Evaluation) (11 ± 5%) and significant degree of coronary artery disease burden, with a mean BCIS-JS of 9 ± 2. Patient characteristics are outlined in Table 1.

Table 1. Patient Characteristics

Age, yrs	67 ± 11
Medical history	
Male	8 (73)
Hypertension	9 (92)
Diabetes mellitus	7 (64)
Hypercholesterolemia	10 (92)
Smokers	6 (54)
BMI, kg/m^2	27 ± 4
Prior MI	11 (100)
Previous PCI	5 (45)
Peripheral vascular disease	4 (36)
Left ventricular ejection fraction, %	34 ± 8
Logistic EuroSCORE, %	11 ± 5
Coronary artery disease	
1-vessel	0 (0)
2-vessel	8 (73)
3-vessel	3 (27)
Left main stem	4 (36)
Left anterior descending	7 (64)
Circumflex	4 (36)
Right coronary artery	5 (45)
BCIS-JS	9 ± 2

Values are mean ± SD or n (%).
BCIS-JS = British Cardiovascular Intervention Society Jeopardy Score; BMI = body mass index; EuroSCORE = European System for Cardiac Operative Risk Evaluation; MI = myocardial infarction; PCI = percutaneous coronary intervention.

Effects of hyperemia on unassisted coronary hemodynamics. Heart rate and aortic and distal coronary pressures remained unchanged during intracoronary adenosine-induced hyperemia (p = 0.41, 0.93, and 0.26, respectively). There was a reduction in microvascular resistance ($R^2 = 0.61$, p = 0.003) with a corresponding increase in coronary flow (APV) ($R^2 = 0.62$, p = 0.01). Furthermore, there was an increase in the microcirculatory BEW ($R^2 = 0.57$, p = 0.02). Table 2 provides a summary of the hemodynamic observations.

IABP effects with "switched on" autoregulation. SYSTEMIC AND PULSE WAVE PARAMETERS. During basal conditions, heart rate remained unchanged following the introduction of IABP device (66.3 ± 14.1 vs. 66.4 ± 12.3 beats/min, p = 0.87). Mean P_a altered significantly with balloon-pump assistance (92.2 ± 16.4 vs. 95.4 ± 20.4 mm Hg, p = 0.03). A nonsignificant trend in reduction of TTI was observed (30.1 ± 15.2 vs. 27.8 ± 13.9, p = 0.08) with balloon augmentation. Whereas the device did not alter the duration of diastole, with diastolic time fraction remaining unchanged (0.65 ± 0.07 vs. 0.64 ± 0.08 s, p = 0.87), diastolic pressure-time index, DTI, increased in conjunction with diastolic augmentation of mean P_a with counterpulsation therapy (43.9 ± 11.9 vs. 54.2 ± 13.4, p = 0.007). The ratio of myocardial oxygen supply (DTI) to demand (TTI), the Buckberg index, increased (1.70 ± 0.68 vs. 2.08 ± 0.57, p = 0.03).

MEAN CORONARY INDICES. Whereas balloon pump augmentation led to an increase in distal coronary pressure (82.4 ± 16.1 vs. 88.7 ± 17.8 mm Hg, p = 0.04), there was no corresponding change in mean flow velocity (APV) (32.3 ± 11.1 vs. 26.6 ± 11.3 cm s^{-1}, p = 0.08) in the presence of a functioning autoregulation. Similarly, velocity time integral remained unchanged during basal IABP-assisted conditions (26.8 ± 12.3 vs. 22.8 ± 7.5 cm, p = 0.51). Microvascular resistance during basal conditions was observed to increase significantly during counterpulsation therapy (2.32 ± 0.5 vs. 3.27 ± 0.41 mm Hg cm s^{-1}, p = 0.001).

CORONARY WAVE INTENSITY ANALYSIS. The 3 previously described wave energies (FCW, backward compression wave, and BEW) were identified in all patients. Figure 2 demonstrates a typical coronary wave intensity profile. Additionally coronary WIA of the circulation during IABP counterpulsation showed 2 additional wave energies (Fig. 3) relating to the inflation and deflation of the balloon. Inflation resulted in an aortic-originating (forward traveling)

Table 2. Hemodynamic Characteristics

	Basal ("Switched On" Autoregulation)			Hyperemic ("Switched Off" Autoregulation)		
	Unassisted	IABP-Assisted	p Value	Unassisted	IABP-Assisted	p Value
Mean-per-beat derivatives						
HR, beats/min	66.3 ± 14.1	66.4 ± 12.3	0.87	69.2 ± 14.2	69.1 ± 12.6	0.85
P_a, mm Hg	92.6 ± 17.4	95.4 ± 20.4	0.03	93.4 ± 16.4	92.1 ± 15.4	0.01
P_d, mm Hg	82.4 ± 16.1	88.7 ± 17.8	0.04	82.4 ± 16.1	89.7 ± 14.4	0.02
APV, cm s^{-1}	32.3 ± 11.1	26.6 ± 11.3	0.08	39.4 ± 10.5*	44.7 ± 17.5†	0.002
MR, mm Hg cm s^{-1}	2.32 ± 0.52	3.27 ± 0.41	0.001	2.11 ± 0.42*	2.25 ± 0.78†	0.45
Pulse wave analysis						
VTI, cm	26.8 ± 12.3	22.8 ± 7.5	0.51	25.8 ± 15.1	32.4 ± 15.7	0.009
DTF	0.65 ± 0.07	0.64 ± 0.08	0.87	0.60 ± 0.09	0.61 ± 0.09	0.33
DTI	43.9 ± 11.9	54.2 ± 13.4	0.007	39.5 ± 13.0	46.5 ± 14.5	0.01
TTI	30.1 ± 15.2	27.8 ± 6.8	0.08	31.4 ± 11.6	27.9 ± 8.7	0.11
BI	1.70 ± 0.68	2.08 ± 0.57	0.03	1.31 ± 0.37	1.91 ± 0.56	0.01
Wave intensity analysis, W m^{-2} s^{-2} × 10^5						
Systolic wave energies						
FCW	+1.70 ± 0.40	+1.82 ± 0.51	0.27	+1.75 ± 0.46	+1.78 ± 0.55	0.34
BCW	−0.32 ± 0.20	−0.55 ± 0.31	0.06	−0.48 ± 0.25	−0.36 ± 0.18	0.17
Diastolic wave energies						
BEW	−2.21 ± 0.64	−1.62 ± 0.67	0.004	−2.43 ± 0.63*	−1.98 ± 0.76†	0.07
IABP-FCW	N/A	+1.82 ± 0.90	N/A	N/A	+1.86 ± 0.67	N/A
IABP-FEW	N/A	+0.95 ± 0.81	N/A	N/A	+0.91 ± 0.76	N/A

*Statistically significant changes in parameters observed during unassisted basal versus hyperemic conditions (APV: p = 0.01; MR: p = 0.003; BEW: p = 0.02). †Statistically significant changes in parameters observed during IABP-assisted basal versus hyperemic conditions (APV: p = 0.005; MR: p = 0.0001; BEW: p = 0.03).

APV = average peak velocity; BCW = backward compression wave; BEW = backward expansion wave; BI = Buckberg index; DTF = diastolic time fraction; DTI = diastolic time integral; FCW = forward compression wave; FEW = forward expansion wave; HR = heart rate; IABP = intra-aortic balloon pump; MR = microvascular resistance; N/A = not applicable; P_a = mean aortic pressure; P_d = mean distal coronary pressure; TTI = tension time index; VTI = velocity time integral.

accelerating compression wave (IABP-FCW), with the subsequent deflation of the balloon causing an aortic-originating (forward traveling) decelerating expansion wave (IABP-FEW). Furthermore, during balloon-pump assistance peak BEW was reduced compared with unassisted conditions (−2.21 ± 0.64 vs. −1.62 ± 0.67 W $m^{-2}s^{-2}$ × 10^5, p = 0.004). During unassisted conditions, the relative acceleratory energies provided by FCW and BEW were 39% and 61%, respectively, whereas during IABP-assistance, FCW was 36%, BEW reduced to 30%, with the IABP-FCW accounting for 34% of total wave energy.

IABP effects with "switched off" autoregulation. SYSTEMIC AND PULSE WAVE PARAMETERS. Balloon counterpulsation during intracoronary adenosine-induced hyperemia did not alter the heart rate (69.2 ± 14.2 vs. 69.1 ± 12.6 beats/min, p = 0.85), diastolic time fraction (0.60 ± 0.09 vs. 0.61 ± 0.09 s, p = 0.33), or mean P_a (93.4 ± 16.4 vs. 92.1 ± 15.4 mm Hg, p = 0.57) compared with unassisted conditions. TTI was reduced (although this was not statistically significant: 31.4 ± 11.6 vs. 27.9 ± 8.7, p = 0.11), and there was an increase in DTI (39.5 ± 13.0 vs. 46.5 ± 14.5, p = 0.01), with a corresponding increase in Buckberg index (1.31 ± 0.37 vs. 1.91 ± 0.56, p = 0.01), mirroring observations during basal conditions.

MEAN CORONARY INDICES. Similar to basal conditions, balloon-pump assistance in the hyperemic setting was accompanied by an increase in distal coronary pressure (82.4 ± 16.1 vs. 89.7 ± 14.4 mm Hg, p = 0.02). However, in contrast to the basal state, there was an increase in APV (39.4 ± 10.5 vs. 44.7 ± 17.5 cm s^{-1}, p = 0.002). Furthermore, velocity time integral was observed to increase during balloon assistance (25.8 ± 15.1 vs. 32.4 ± 15.7, p = 0.009). Hyperemic microvascular resistance was unchanged in unassisted and assisted conditions (2.21 ± 0.42 vs. 2.25 ± 0.78 mm Hg cm s^{-1}, p = 0.45).

CORONARY WAVE INTENSITY ANALYSIS. Augmentation of coronary flow with balloon counterpulsation ($\Delta APV = APV_{IABP} - APV_{unassisted}$) related proportionately with the IABP-FCW wave energy (p = 0.001, R^2 = 0.71) (Fig. 4) with maximal hyperemia; there was no relationship between these parameters in basal conditions. IABP-FEW also related with augmentation of APV (p = 0.003, R^2 = 0.60). Multiple linear regression, confirmed that augmentation in APV was primarily as a result of IABP-FCW (p = 0.01) rather than IABP-FEW (p = 0.14), with $\Delta APV = 2.2 \times 10^{-5}(FEW) + 5.7 \times 10^{-5}(FCW) + 6.13$. The dominant microcirculatory wave, BEW, tended to

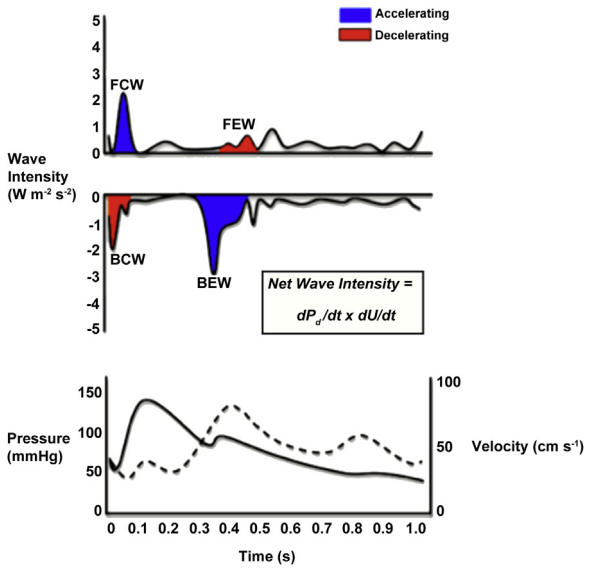

Figure 2. Coronary Wave Intensity Profile

Demonstrates the 4 predominating wave energies present during a single cardiac cycle, with the relative phasic coronary pressure and velocity trends shown below the wave intensity analysis profile. BCW = backward compression wave; BEW = backward expansion wave; FCW = forward compression wave; FEW = forward expansion wave.

decrease during hyperemic balloon-pump assistance (2.43 ± 0.63 vs. 1.98 ± 0.76 W m^{-2} s^{-2} × 10^5, p = 0.07) compared with unassisted conditions.

Discussion

We have comprehensively characterized the effects of intra-aortic balloon counterpulsation on coronary and microvascular hemodynamics, including the first clinical application of coronary WIA in this setting. Using these techniques, we have shown that the effects of IABP therapy are intimately linked to innate microvascular function and that the processes of autoregulation may ameliorate the potential benefits of this therapy. However, when autoregulation is disabled, IABP therapy was seen to augment myocardial perfusion. These findings help to explain the results of recent randomized control trials of balloon counterpulsation and also indicate the potential utility of this therapy in clinical scenarios accompanied by exhausted microcirculatory reserve.

Coronary autoregulation and IABP. Coronary blood flow is tightly controlled and matched to the oxygen demands of the heart by adapting the caliber of the coronary resistance arteries, via inter-related processes involving mechanisms intrinsic to the vascular wall, as well as metabolic and neurohumoral factors (22,23). The 2 major determinants of coronary flow are coronary arterial pressure and myocardial oxygen consumption. Coronary autoregulation is the mechanism that maintains coronary flow independent of arterial pressure for a given level of oxygen consumption or changing oxygen requirements at a constant perfusion pressure (24). In the presence of an epicardial coronary stenosis there is intramural microcirculatory vasodilation, reduction in resistance, accommodating for the reduction in pressure distal to the stenosis (25). Ischemia ensues as a result of the inability of this vasodilatory response to match the oxygen requirements, because the threshold of maximal microcirculatory vasodilation has been exceeded, and resistance cannot be reduced any further. Therefore in the presence of persistent ischemia, the autoregulatory mechanisms are completely exhausted, so that myocardial flow becomes proportional to perfusion pressure. This condition of minimal resistance is mimicked by pharmacological administration of adenosine, which causes maximal vasodilation and reduction in microvascular resistance, switching "off" the normal autoregulatory pathways. During this state, we have demonstrated that IABP therapy leads to an increase in distal coronary pressure, which proportionately increases coronary flow. However, when autoregulation is intact, the counterpulsation-related increase in P_d is accompanied by an increase in microvascular resistance, as a consequence of which coronary flow remains unchanged.

Clinical data on IABP efficacy and the impact of autoregulation. The efficacy of IABP therapy has come in to question in recent years in light of several randomized control trials that have failed to demonstrate the efficacy of routine IABP placement in different clinical settings. The first of these was BCIS-1 (4), in which IABP was deployed in patients who were hemodynamically stable at the outset, but were at increased risk of major complications during PCI, who showed no reduction in incidence of major adverse cardiovascular and cerebrovascular events, compared with those randomized to have unassisted PCI. Given that most patients enrolled in BCIS-1 are likely to have had perfusion pressures within the autoregulatory range and that patients with active ischemia and shock were excluded, the findings of the current study may explain why a strategy of routine IABP placement in unselected patients failed to show benefit. On the other hand, 1 in 8 patients who were randomized to receive unsupported PCI experienced hemodynamic compromise sufficient to warrant rescue IABP insertion. There is a signal that those requiring "bail-out" may be patients at the extreme end of the spectrum of diminished physiological reserve, severity of coronary artery disease, and therefore microvascular dysfunction. The CRISP AMI (Counterpulsation to Reduce Infarct Size Pre-PCI Acute Myocardial Infarction) trial (26) assessed the role of routine use of IABP in patients presenting with large anterior STEMIs within 6 h of symptom onset without cardiogenic shock. Pre-procedure IABP insertion failed to reduce infarct size in this study. Although this result

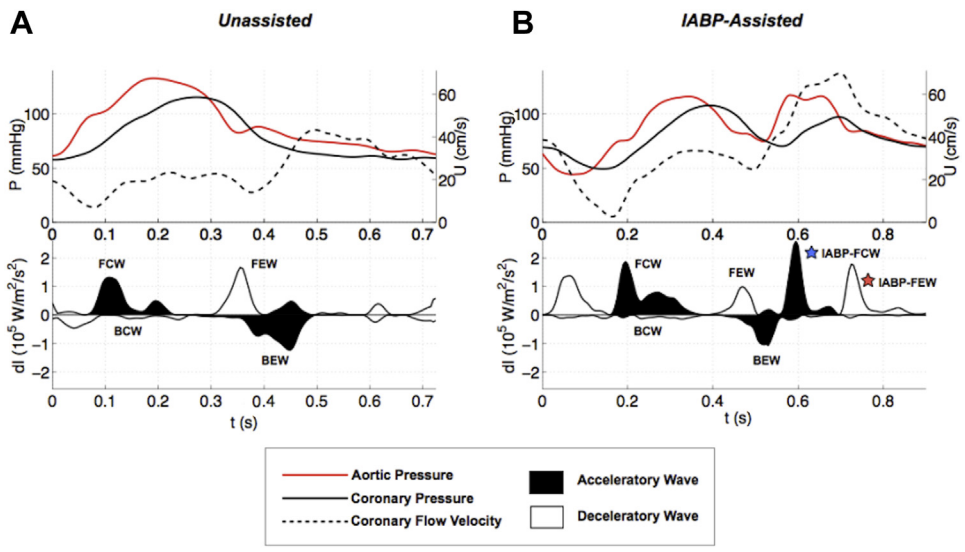

Figure 3. IABP Wave Intensity Profile

(A) Wave intensity analysis profile during unassisted conditions demonstrating the 4 wave energies described in Figure 2. **(B)** Wave intensity analysis profile during intra-aortic balloon pump (IABP)-assisted conditions, highlighting the temporally related wave energies with device inflation (IABP-FCW) and deflation (IABP-FEW). Both obtained with autoregulation "switched off" during hyperemia. Abbreviations as in Figure 2.

appears to be at odds with the physiological observations seen in the current study, this lack of effect may have been due to the relatively brief period of counterpulsation prior to mechanical reperfusion being achieved. From our observations, the subgroup who stands to gain most benefit from counterpulsation therapy may be the one that had persisting ischemia despite reperfusion. Analysis of this subset of patients in CRISP-AMI may be instructive.

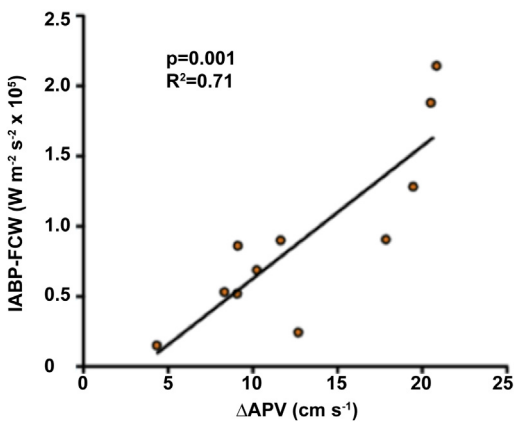

Figure 4. IABP-FCW Relationship With Hyperemic Coronary Flow Velocity

During hyperemia, with autoregulation disabled, IABP device inflation is associated with an acceleratory wave energy (IABP-FCW) that is linearly related to coronary flow (average peak velocity [APV]). Abbreviations as in Figures 2 and 3.

The most recent of these randomized clinical trials was IABP-SHOCK II (Intra-aortic Balloon Support for Myocardial Infarction With Cardiogenic Shock) (6), which assessed the utility of IABP in acute myocardial infarction complicated by cardiogenic shock. A strategy of elective IABP insertion failed to reduce 30-day mortality in this study. Although hypotension is central to the clinical diagnosis of cardiogenic shock, it is interesting to note that systolic blood pressure was in excess of 90 mm Hg in approximately 50% of all patients enrolled in IABP-SHOCK II, falling within the normal range of coronary autoregulation. Applying the observations of our current study, it could be postulated that the presence of a working autoregulatory system may have limited the effect of IABP therapy in many patients of the IABP-SHOCK II cohort.

The effect of autoregulation on the efficacy of mechanical hemodynamic support may also be applicable to devices that aim to directly unload the left ventricular cavity. Remmelink et al. (27) previously observed in a cohort of patients undergoing PCI with left ventricular dysfunction with adjunctive Impella device (Cardiotechnik, Aachen, Germany) support that during basal conditions, increased distal coronary pressure did not lead to an augmentation of coronary flow, though a linear increase was evident during hyperemic conditions. Analogous with the current study, an increase in basal microvascular resistance, due to the presence of a functioning microcirculatory autoregulation, diminished the beneficial effect of the device.

Wave intensity analysis of IABP counterpulsation. Kolyva et al. (28,29) previously demonstrated the effect of the IABP balloon on aortic hemodynamics during in vivo and ex vivo experiments, delineating the unique ability of WIA in assessing the hemodynamic effects of the device, highlighting the relationship of device inflation and deflation to wave propagation in the aorta. The current study represents the first application of WIA to pressure and flow measurements in the coronary circulation during counterpulsation in humans. We have demonstrated that IABP therapy is associated with a characteristic WIA morphology, with 2 unique diastolic waves observed, the first, a further FCW, corresponds with inflation of the balloon, and the second with balloon deflation. These novel parameters allow comprehensive assessment of the effects of IABP therapy integrated with innate microvascular and contractile function and may prove to be useful in future counterpulsation research, aimed at distinguishing responders from nonresponders and for assessing the relative efficacy of newer iterations of pulsatile assist devices.

Using these techniques, we have demonstrated that IABP augmentation of aortic and distal coronary pressure does not necessarily translate to an improvement in coronary flow or perfusion of the heart, as previously thought. Instead, we have shown that the energy driving myocardial perfusion during counterpulsation is entirely different to the patterns in unassisted conditions, with the added beneficial energy of the IABP-FCW being offset by a decrease in the BEW (in turn due to an increase in microvascular resistance due to autoregulation) such that net coronary flow remains unchanged. In contrast, during hyperemic conditions, when autoregulation is disabled, there is no diminution of the BEW during counterpulsation, such that the effect of the IABP-FCW and the BEW are summative, resulting in augmentation of coronary flow. In the presence of

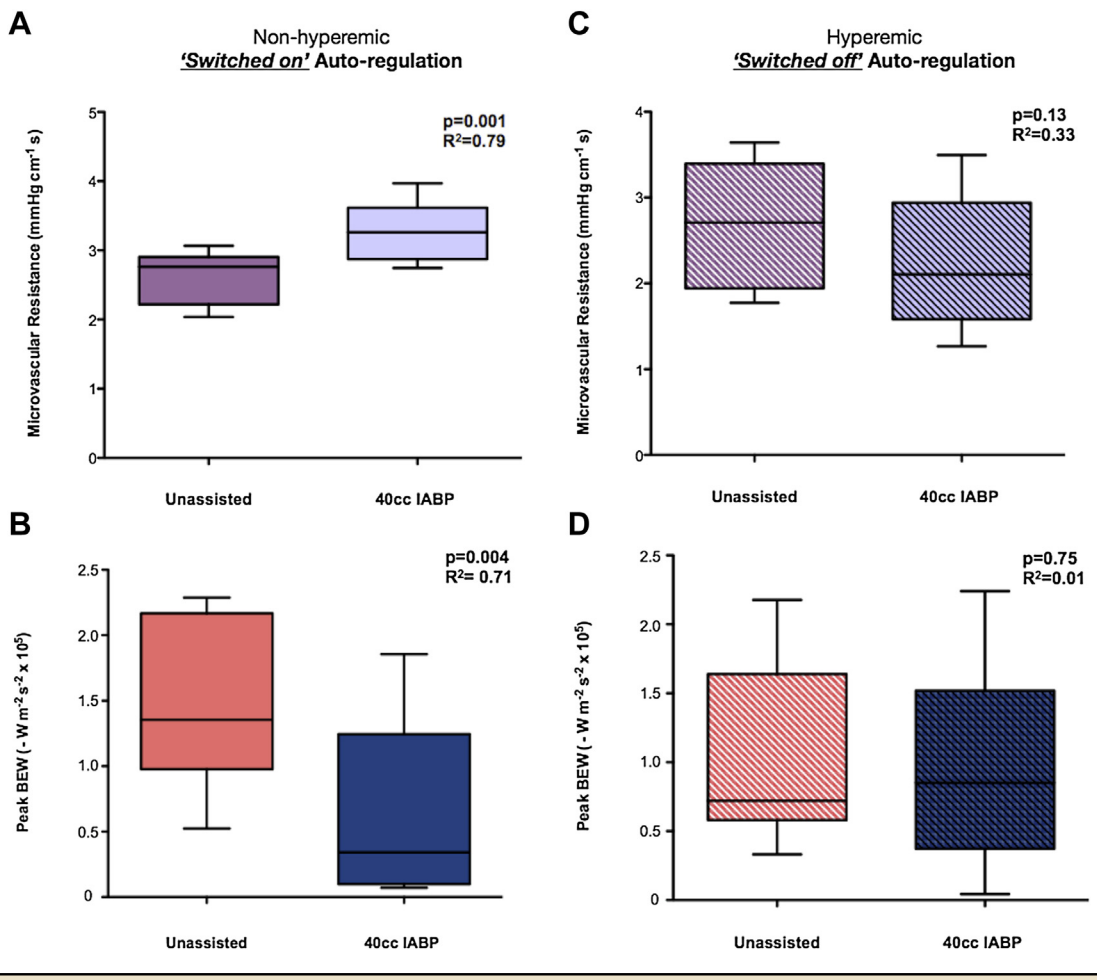

Figure 5. Relationship of MR With Microcirculatory BEW

(A, B) Microvascular resistance (MR) and BEW during basal conditions. **(C, D)** MR and BEW in hyperemia. Abbreviations as in Figures 2 and 3.

hyperemia, the energy from the balloon inflation (IABP-FCW) related linearly to the increase in peak coronary flow velocity (ΔAPV) (Fig. 5). These observations may explain the lack of benefit seen when the IABP is employed prophylactically rather than in cases when autoregulatory mechanisms have been rendered dysfunctional, such as in the presence of persistent ischemia or shock.

We have described a novel experimental model to characterize the effects of intra-aortic balloon counterpulsation on myocardial perfusion and to compare its efficacy in 2 settings, with and without functioning autoregulation. These techniques have the potential to be applied to investigation of other circulatory assist devices, including those that allow direct left ventricular unloading and iterations of the balloon pump itself, in a variety of clinical and experimental settings.

Study limitations. This was a small, single center study, but it is the first in human study to describe the relationship and effects of the use of intra-aortic balloon counterpulsation on coronary wave intensity and the effects of modulating coronary autoregulation on the utility of IABP therapy. As a consequence of the small sample sizes and the use of unadjusted statistical tests adopted within the studies, there is potential for a type 1 error affecting the results. Therefore, further investigation is warranted to confirm these initial findings.

Conclusions

Autoregulation ameliorates the effect of IABP on coronary flow by increasing microvascular resistance in response to increased distal coronary pressure. However, during hyperemic conditions, IABP augments myocardial perfusion, principally due to a diastolic FCW caused by balloon inflation. These findings suggest IABP will be of greatest benefit when regional microcirculatory reserve is exhausted.

Reprint requests and correspondence: Dr. Divaka Perera, Cardiovascular Division, The Rayne Institute, St. Thomas's Hospital, 123 Coldharbour Lane, London SE1 7EH, United Kingdom. E-mail: Divaka.Perera@kcl.ac.uk.

REFERENCES

1. Grayson AD, Moore RK, Jackson M, et al., for the North West Quality Improvement Programme in Cardiac Interventions Investigators. Multivariate prediction of major adverse cardiac events after 9914 percutaneous coronary interventions in the north west of England. Heart 2006;92:658–63.
2. Moscucci M, Kline-Rogers E, Share D, et al. Simple bedside additive tool for prediction of in-hospital mortality after percutaneous coronary interventions. Circulation 2001;104:263–8.
3. Wallace TW, Berger JS, Wang A, Velazquez EJ, Brown DL. Impact of left ventricular dysfunction on hospital mortality among patients undergoing elective percutaneous coronary intervention. Am J Cardiol 2009;103:355–60.
4. Perera D, Stables R, Thomas M, et al., for the BCIS-1 Investigators. Elective intra-aortic balloon counterpulsation during high-risk percutaneous coronary intervention: a randomized controlled trial. JAMA 2010;304:867–74.
5. Patel MR, Smalling RW, Thiele H, et al. Intra-aortic balloon counterpulsation and infarct size in patients with acute anterior myocardial infarction without shock: the CRISP AMI randomized trial. JAMA 2011;306:1329–37.
6. Thiele H, Zeymer U, Neumann FJ, et al., for the IABP-SHOCK II Trial Investigators. Intraaortic balloon support for myocardial infarction with cardiogenic shock. N Engl J Med 2012;367:1287–96.
7. Fearon WF, Shah M, Ng M, et al. Predictive value of the index of microcirculatory resistance in patients with ST-segment elevation myocardial infarction. J Am Coll Cardiol 2008;51:560–5.
8. Kitabata H, Imanishi T, Kubo T, et al. Coronary microvascular resistance index immediately after primary percutaneous coronary intervention as a predictor of the transmural extent of infarction in patients with ST-segment elevation anterior acute myocardial infarction. J Am Coll Cardiol Img 2009;2:263–72.
9. De Silva K, Foster P, Guilcher A, et al. Coronary wave energy: a novel predictor of functional recovery after myocardial infarction. Circ Cardiovasc Interv 2013;6:166–75.
10. Davies JE, Whinnett ZI, Francis DP, et al. Evidence of a dominant backward-propagating "suction" wave responsible for diastolic coronary filling in humans, attenuated in left ventricular hypertrophy. Circulation 2006;113:1768–78.
11. Davies JE, Sen S, Broyd C, et al. Arterial pulse wave dynamics after percutaneous aortic valve replacement: fall in coronary diastolic suction with increasing heart rate as a basis for angina symptoms in aortic stenosis. Circulation 2011;124:1565–72.
12. Spaan JA, Breuls NP, Laird JD. Diastolic-systolic coronary flow differences are caused by intramyocardial pump action in the anesthetized dog. Circ Res 1981;49:584–93.
13. Krams R, Sipkema P, Westerhof N. Varying elastance concept may explain coronary systolic flow impediment. Am J Physiol 1989;257:H1471–9.
14. Wiggers CJ. The interplay of coronary vascular resistance and myocardial compression in regulating coronary flow. Circ Res 1954;2:271–9.
15. De Silva K, Morton G, Sicard P, et al. Prognostic utility of BCIS Myocardial jeopardy score for classification of coronary disease burden and completeness of revascularization. Am J Cardiol 2013;111:172–7.
16. Califf RM, Phillips HR 3rd, Hindman MC, et al. Prognostic value of a coronary artery jeopardy score. J Am Coll Cardiol 1985;5:1055–63.
17. Savitzky A, Golay MJE. Smoothing and differentiation of data by simplified least squares procedures. Anal Chem 1964;36:1627–39.
18. Parker KH, Jones CJ. Forward and backward running waves in the arteries: analysis using the method of characteristics. J Biomech Eng 1990;112:322–6.
19. Davies JE, Whinnett ZI, Francis DP, et al. Use of simultaneous pressure and velocity measurements to estimate arterial wave speed at a single site in humans. Am J Physiol Heart Circ Physiol 2006;290:H878–85.
20. Buckberg GD, Fixler DE, Archie JP, Hoffman JI. Experimental subendocardial ischemia in dogs with normal coronary arteries. Circ Res 1972;30:67–81.
21. Meuwissen M, Chamuleau SA, Siebes M, et al. Role of variability in microvascular resistance on fractional flow reserve and coronary blood flow velocity reserve in intermediate coronary lesions. Circulation 2001;103:184–7.
22. Komaru T, Kanatsuka H, Shirato K. Coronary microcirculation: physiology and pharmacology. Pharmacol Ther 2000;86:217–61.
23. Bassenge E, Heusch G. Endothelial and neuro-humoral control of coronary blood flow in health and disease. Rev Physiol Biochem Pharmacol 1990;116:77–165.
24. Mosher P, Ross J Jr., McFate PA, Shaw RF. Control of coronary blood flow by an autoregulatory mechanism. Circ Res 1964;14:250–9.

25. Siebes M, Verhoeff BJ, Meuwissen M, de Winter RJ, Spaan JA, Piek JJ. Single-wire pressure and flow velocity measurement to quantify coronary stenosis hemodynamics and effects of percutaneous interventions. Circulation 2004;109:756–62.
26. Patel MR, Smalling RW, Thiele H, et al. Intra-aortic balloon counterpulsation and infarct size in patients with acute anterior myocardial infarction without shock: the CRISP AMI randomized trial. JAMA 2011;306:1329–37.
27. Remmelink M, Sjauw KD, Henriques JP, et al. Effects of left ventricular unloading by Impella recover LP2.5 on coronary hemodynamics. Catheter Cardiovasc Interv 2007;70:532–7.
28. Kolyva C, Pantalos GM, Giridharan GA, Pepper JR, Khir AW. Discerning aortic waves during intra-aortic balloon pumping and their relation to benefits of counterpulsation in humans. J Appl Physiol 2009; 107:1497–503.
29. Kolyva C, Pantalos GM, Pepper JR, Khir AW. How much of the intraaortic balloon volume is displaced toward the coronary circulation? J Thorac Cardiovasc Surg 2010;140:110–6.

Key words: intra-aortic balloon pump ■ left ventricular dysfunction ■ microvascular function ■ wave intensity analysis.